Electronic Structure of LaF^+ and LaF from Frozen-Core Four-Component Relativistic Multiconfigurational Quasidegenerate Perturbation Theory

Hiroko Moriyama,[†] Yoshihiro Watanabe,[‡] Haruyuki Nakano,[‡,§] and Hiroshi Tatewaki*[,†]

Graduate School of Natural Sciences, Nagoya City University, Nagoya, Aichi 467- 8501, Japan, Department of Chemistry, Faculty of Sciences, Kyushu University, Fukuoka 812- 8581, Japan, and CREST, Japan Science and Technology Agency (JST), Kawaguchi, Saitama 332- 0012, Japan

Received: October 2, 2007; In Final Form: December 21, 2007

The electronic structure of the molecules LaF^+ and LaF was studied using frozen-core four-component multiconfigurational quasidegenerate perturbation theory. To obtain proper excitation energies for LaF^+, it was essential to include electronic correlations between the outermost valence electrons (4f, 5d, and 6s) and ionic core electrons composed of (4s, 4p, 4d, 5s, and 5p). The lowest-lying 16 excited states were examined for LaF^+, and the lowest 30 states were examined for LaF. The excitation energies calculated for LaF^+ agree with the available experimental values, as well as with values from ligand field theory. Errors are within 0.4 eV; for example, the highest observed state $^2\Pi$ is 3.77 eV above the ground state, and the present value is 4.09 eV. For LaF, agreement between the experimental and theoretical state assignments and between the experimental and calculated excitation energies was generally good, except for the electron configurations of certain states. Errors are within 0.4 eV except for a single anomaly; for example, the highest observed excited-state discussed in this work is 2.80 eV above the ground state, and the present value is 2.42 eV. We discuss the characteristics of the bonding in LaF^+ and LaF.

1. Introduction

LaF^+ and LaF can be studied either as a transition metal fluoride or as a lanthanide metal fluoride. Experimentally, Shenyavskaya and Gurvich[1] found the ground state of LaF^+ to be $(6s)^1\ ^2\Sigma$. Kaledin, Kaledin, and Heaven[2] then asserted that the ground state is $(5d)^1\ ^2\Delta$ with $\Omega = 1.5$, using laser adsorption spectra and ligand field theory (LFT). The excited states of this ion were studied extensively by these authors. Because LaF^+ is the simplest lanthanide monofluoride, we investigate it in depth as a basis for discussing the electronic structure of the larger lanthanide compounds. We study it here using four-component relativistic theory. It was necessary to include electronic correlations between the valence and ion cores, including the 4s, 4p, and 4d electrons, to give the appropriate designations for the excited states; see Section 3.

The LaF visible band was first studied by Barrow, Bastin, and Moore.[3] Schall, Linton, and Field[4] identified the ground state as $(6s)^2\ ^1\Sigma$. Since then, there have been many experimental studies of the excited states.[5−11] (A review of spectroscopic properties of rare earths is given in ref 12.) Only three theoretical works have been published for LaF, however. Schall, Dulick, and Field[13] discussed the excited states of LaF using LFT. Hong, Dolg, and Li[14] gave the spectroscopic constants for lanthanide monoxides and monofluorides including LaF, using the scalar-relativistic zeroth-order regular approximation and Douglas−Kroll−Hess approximation. Fahs and co-workers[15] investigated the excited states of LaF. In their calculation, 46 core electrons in La are treated via pseudopotentials, and the actual number of electrons is 20 (= La $5s^25p^65d^16s^2$ + F $1s^22s^22p^5$). Of these, 8 electrons (La $5d^16s^2$ + F $2p^5$) were selected as active, and the remaining 12 were frozen. Fahs and co-workers[15] performed complete-active-space self-consistent-field (CASSCF) calculations with 12 active molecular orbitals assembled from s and d atomic orbitals. After CASSCF, multireference configuration interaction (CI) calculations were performed to account for correlation effects. Spin−orbit effects were introduced semiempirically.[15] Configurations including the 6p spinors are disregarded in their calculations. Although the resulting excitation energies generally agree with experiment, the present work will demonstrate that the contributions of the La 6p spinors are significant in some excited states assigned as $(5d^16s^1)$.

We know of no investigations using four-component relativistic theory. We therefore studied LaF using the four-component relativistic theory, to establish the designations for the excited states. The calculated excitation energies generally agree with those of experiment but in some states contradict the experimental electronic configuration.[4]

We also discuss the characteristics of the chemical bond of LaF^+ and LaF. For example, LaF is considered to be the ionic compound La^+F^-. In the atomic ion, the electronic configuration of the La^+ ground state is $(5d)^2$, but the electronic configuration of the ground state of LaF is $(6s)^2$-like. We shall explain this.

Section 2 sets out the method of the calculations. Section 3 then discusses the electronic structure of LaF^+ and LaF. Section 4 offers concluding remarks.

2. Method of the Calculation

2.1. RFCA and Basis Set. Because it is difficult to treat all 57 of the electrons of the La atom, we used the reduced frozen-core approximation (RFCA) proposed by Matsuoka and Watanabe.[16,17] We prepared four ionic cores for the La atom, because in the preliminary calculations the errors given by the

* Author to whom correspondence should be addressed. E-mail: htatewak@nsc.nagoya-cu.ac.jp.
† Nagoya City University.
‡ Kyushu University.
§ CREST, Japan Science and Technology Agency (JST).

10.1021/jp7096197 CCC: $40.75
Published on Web 03/01/2008

large core, ordinarily accepted as appropriate (see C1 and C2 below), lead to large errors in the calculated excitation energies. We categorize electrons into three sets: frozen-core (f-core) electrons; active-core (a-core) electrons from which one and two electron excitations are allowed but are not treated as valence electrons in CASCI; and the valence electrons (val.)

C1, f-core {Cd (48) + He (2)} + a-core {$(5p^6)+(2s^22p^6)$} + val.;

C2, f-core {Pd (46) + He (2)} + a-core {$(5s^25p^6)+(2s^22p^6)$} + val.;

C3, f-core {Kr (36) + He (2)} + a-core {$(4d^{10}5s^25p^6)+(2s^2-2p^6)$} + val.;

C4, f-core {Zn^{2+}(28) + He (2)} + a-core {$(4s^24p^64d^{10}5s^2-5p^6)+(2s^22p^6)$} + val.;

As an example, the notation "f-core {Cd (48) + He (2)}" indicates that the frozen-core is composed of a Cd-like ion core in La, having 48 electrons, and a He-like ion core in F, having 2 electrons that are fixed to the atomic spinors. Also "a-core {$(5p^6)$ + $(2s^2\ 2p^6)$}" indicates that the active-core is composed of La($5p^6$) and F($2s^22p^6$). The number of active electrons for C1−C4 is 14−34. The number of valence electrons is 1 or 2 depending on whether LaF^+ or LaF is treated. The basis set for the respective calculations of C1−C4 are rather large. For example, the set for C4 is La[1*6/1*5+(11)/1*7/1*8/(1)] + F[21/422/(1)], where a slash separates the symmetries s, p, d, f, and g symmetries, 1*n implies that n primitive Gaussian type functions (pGTFs) are used, and a 2 and 4 indicate that the contracted GTFs (cGTF) are spanned with 2 and 4 primitives, respectively. The (11) and (1) for La are two p-type polarization functions[18] and one g-type polarization function, whereas (1) for F is a single d-type polarization function.[18] The total number of molecular spinors generated is 145.

The La pGTFs in the parentheses are those of the most diffuse GTFs in the respective atomic spinors given by Koga, Tatewaki, and Matsuoka (KTM).[19] The 8 f-type primitives are generated in the present work. The La p-type polarization functions have a similar diffuseness (exponents are 0.041, 0.012) to that of the s-type pGTFs for the 6s atomic spinor (exponents are 0.055, 0.023), so that we have not added further p primitives. For the F a-core, cGTFs are constructed from the atomic spinors given by KTM.[20]

2.2. Complete Active Space Configuration Interaction (CASCI) and Multiconfigurational Quasidegenerate Perturbation Theory (MC-QDPT). *2.2.1. LaF^+.* For LaF^+, we first performed RFCA Dirac−Fock−Roothaan (DFR) calculations for LaF^{2+}. $\{La^{3+}(5p^6)F^-(2p^6)\}^{2+}$ provides appropriate valence spinors for the LaF^+ ground and excited states, having the electronic configurations $(LaF)^{2+}nl^1$, because LaF^{2+} gives the electronic field generated by the m (m = 14−34) active-core electrons, which equivalently acts on the virtual spinors in which a nl electron moves. In the next section, we shall see the adequateness of the resulting spinors for LaF^+. Second, assuming the no virtual pair approximation,[21−26] we performed CASCI[27,28] calculations using LaF^{2+} virtual (valence) spinors, filling one electron in the respective spinors. Third, to account for electron correlation effects among the valence electrons and between the valence and active-core electrons, we performed MC-QDPT[28] calculations. The matrix element of MC-QDPT is expressed as

$$H_{\mu\nu} = E_\mu^{GCS-CI}\,\delta_{\mu\nu} + \frac{1}{2}\sum_{I\notin GCS}\left\{\frac{<\mu\mid H_{DC}^{+}\mid I><I\mid H_{DC}^{+}\mid \nu>}{E_\nu^{(0)}-E_I^{(0)}} + H.C.\right\} \quad (1)$$

where μ and ν denote CASCI eigenfunctions. The one and two electron excitations from the active-core and valence shells to all the valence and virtual spinors (denoted as I) were taken into account where the CSFs included in the CASCI are excluded.[28] We did not encounter intruder states[29−31] in this work. The appropriateness of the core C1−C4 is tested, calculating the excitation energies. It emerges that the smallest core, C4, is needed. Moreover, CAS space spanned with the lowest 30 virtual spinors of LaF^{2+} was found to be necessary to obtain reasonable excitation energies.

2.2.2. LaF. For LaF, using the C4 model, we performed RFCA DFR calculations for LaF^+, then performed CASCI, filling 2 electrons in the lowest 30 virtual (valence) molecular spinors. Because Zn^{2+} + He cores are used, it is taken into account the correlation effects between the 2 valence and 34 active-core electrons in MC-QDPT. We scarcely met intruder states[29−31] as in LaF^+.

The present MC-QDPT program treats distinctly the two strings of subspecies due to time reversal symmetry; for example, we actually used 60 valence spinors rather than 30 spinors.

2.3. Spectroscopic Constants. Using the potential curves given by MC-QDPT, we obtained the spectroscopic constants of R_e and ω_e and excitations of T_e (electronic transition energies between the two potential minima) and T_0 (electronic transition energies between the corresponding 0 vibrational energies) by solving the one-dimensional Schrödinger equation using the Numerov method;[32,33] the potential curves are fitted to the fifth-degree polynomial of internuclear distance R, and ω_e, $\omega_e x_e$, and $\omega_e y_e$ are determined using the lowest three vibrational states of the respective symmetries. We compiled only ω_e in this work.

3. Results

3.1. LaF^+. *3.1.1. DFR Calculation.* Because it is considered that the LaF^{2+} ion provides appropriate molecular spinors for various LaF^+ electronic states including the ground state, we first performed DFR calculations for the LaF^{2+} ion, using the four La ion core models listed in Section 2.1. Although we have not shown detailed results with these cores except for C4, the respective core models gave similar energetics so far as DFR is concerned; the total energies are similar, irrespective of the ion core size, and the same is true for the occupied and virtual spinors. For example, the DFR total energies for LaF^{2+} given at R = 3.75 bohrs (1.984 Å) by C1, C2, C3, and C4 are −8592.7503, −8592.7525, −8592.7522, and −8592.7507 hartrees, respectively, and the highest occupied spinors having characteristics of F $(2p_+)_{1/2}$ are −1.0054, −1.0066, −1.0068, and −1.0070 hartrees, respectively. The spinor energies and gross atomic orbital populations for C4 are shown in Table 1, and the contour maps for the important spinors are displayed in Figure 1. The total electron number in La is 26.5, and for F is 7.5. Formally, atomic La^{2+} takes the electronic configuration $(4s^24p^64d^{10}5s^25p^65d^1)$, including 27 electrons, and F is $(2s^2-2p^5)$ including 7 electrons. From Table 1, we see in LaF^{2+} that 0.5 La 5d electrons move into F 2p spinors to form $\{La^{2.5+}-(5p^6d^{*0.4}f^{*0.1})F^{0.5-}(2p^{5.5})\}^{2+}$, where d* and f* are the polarization functions of La that form molecular spinors with F 2ps. A single valence electron in LaF^+ thus moves in the field generated by $\{La^{2.5+}(5p^6d^{*0.4}f^{*0.1})F^{0.5-}(2p^{5.5})\}^{2+}$.

We may find a similar charge transfer in LaF^+ DFR, suggesting that the chemical bonding in LaF arises from charge transfer from the La^{2+} ion to the F atom (see Section 3.3).

3.1.2. Verification of the Appropriateness of the Ion Core. When performing CASCI, we should determine the number of

TABLE 1: Spinor Energies (hartrees) and GAOPS of LaF^{2+} at $R = 2.002$ Å with C4[a,b]

no.	spnr energy	Ω	La s_+	La p_-	La p_+	La d_-	La d_+	La f_-	La f_+	F s_+	F p_-	F p_+
10	−2.3205	1/2	1.951	0.000	−0.001	0.000	0.000	0.000	0.000	0.039	0.004	0.007
11	−1.9513	1/2	0.038	0.064	0.082	0.005	0.007	0.002	0.002	1.775	0.008	0.017
12	−1.6066	1/2	0.001	1.887	0.041	0.002	0.000	0.000	0.000	0.051	0.000	0.018
13	−1.5148	3/2	0.000	0.000	1.989	0.000	0.000	0.000	0.000	0.000	0.000	0.011
14	−1.4989	1/2	0.004	0.014	1.773	0.002	0.005	0.000	0.001	0.113	0.046	0.043
15	−1.0115	1/2	0.000	0.007	0.007	0.051	0.044	0.022	0.019	0.000	1.303	0.545
16	−1.0092	3/2	0.000	0.000	0.015	0.020	0.077	0.012	0.029	0.000	0.000	1.846
17	−1.0024	1/2	0.014	0.028	0.081	0.087	0.112	0.018	0.022	0.013	0.469	1.155
$\sum GAOP_{i\lambda}(i = 1,17)$			4.007	4.001	7.987	4.167	6.246	0.054	0.072	1.990	1.830	3.643
total GAOP for a-core						La: 26.534					F:7.467	
18	−0.3906	3/2	0.000	0.000	0.000	1.662	0.330	0.006	0.001	0.000	0.000	0.000
19	−0.3889	1/2	1.662	0.021	0.042	0.117	0.148	0.001	0.001	0.000	0.003	0.007
20	−0.3872	5/2	0.000	0.000	0.000	0.000	1.992	0.001	0.007	0.000	0.000	0.000
21	−0.3610	1/2	0.002	0.121	0.038	1.107	0.596	0.054	0.034	0.000	0.028	0.019
22	−0.3584	3/2	0.000	0.000	0.146	0.276	1.437	0.026	0.068	0.000	0.000	0.048
23	−0.3236	1/2	0.112	0.219	0.356	0.348	0.762	0.055	0.101	−0.008	0.023	0.033
24	−0.2783	1/2	0.001	1.170	0.603	0.078	0.034	0.082	0.026	0.000	0.002	0.004
25	−0.2748	3/2	0.000	0.000	1.791	0.019	0.084	0.030	0.071	0.000	0.000	0.004
26	−0.2330	1/2	0.102	0.268	0.688	0.042	0.081	0.371	0.459	−0.011	0.000	0.001
27	−0.2061	5/2	0.000	0.000	0.000	0.000	0.000	1.945	0.055	0.000	0.000	0.000
28	−0.2012	7/2	0.000	0.000	0.000	0.000	0.000	0.000	2.000	0.000	0.000	0.000
29	−0.2012	3/2	0.000	0.000	0.001	0.007	0.000	1.578	0.413	0.000	0.000	0.000
30	−0.1975	5/2	0.000	0.000	0.000	0.000	0.007	0.054	1.939	0.000	0.000	0.000

[a] This is R_e of the LaF^+ ground state from C4 MC-QDPT; the DFR total energy for LaF^{2+} is -8592.749625 hartrees. [b]The lower first to ninth spinors and the higher 31st to 145th spinors are not shown to save space.

valence spinors which the valence electron occupies. In the Dirac−Fock procedure, any spinors with the same Ω mix with each other; in many cases, we cannot distinguish the spinors purely as s, p, d, and f atomic spinors. The s, p, d, and f atomic spinors yield 7, 5, 3, and 1 molecular spinors for the $\Omega = 1/2$, 3/2, 5/2, and 7/2 symmetries, respectively. If we select the 16 lowest virtual spinors in $\{La^{2.5+}(5p^6d^{*0.4}f^{*0.1})F^{0.5-}(2p^{5.5})\}^{2+}$, then we may include all the necessary atomic spinors, but we select 19 spinors for safety; these are composed of 9, 6, 3, and 1 spinors for the $\Omega = 1/2$, 3/2, 5/2, and 7/2 symmetries.

We then performed MC-QDPT calculations using the C1−C4 core models. The number of valence electrons in LaF^+ is 1, and we recall the numbers in the active-core for C1−C4 is 14−34. The electronic excitation energies (T_0) with MC-QDPT are given in columns 3−6 of Table 2 and can be compared with the experimental values in the final column. Irrespective of the core models, the calculated ground state is always $(5d)_{3/2}^1$, similar to atomic La^{2+} (see the 18th spinor in Table 1 and Figure 1), which is consistent with experiment; the subscript 3/2 and the superscript 1, respectively, denote the total electronic angular momentum Ω of the spinor under consideration and the number of electrons in $(5d)_{3/2}$.

We note the excitation energies for $(4f)_{5/2}^1$ and $(4f)_{7/2}^1$ (see 27th and 28th spinors in Table 1 and Figure 1) because the electronic spectra including f electrons have particular importance in lanthanide chemistry. The calculated excitation energies with C1 are 3.32 and 3.53 eV, which are far from the experimental values of 2.05 and 2.12 eV, but they gradually approach the experimental values as the core varies from C1 to C4. The best is given by C4, which is reasonable because the atomic 4f spinors occupy the same special region as the atomic 4d, 4p, and 4s spinors (as shown in Figure 2), and all of them are included in C4. The calculated excitation energies for $(4f)_{5/2}^1$ and $(4f)_{7/2}^1$ with C4 are 2.10 and 2.41 eV, closer to the experimental values of 2.05 and 2.12 eV. We believe that the calculated excitation energy for $(4f)_{7/2}^1$ is a little larger. We therefore expand the spinor space included in CASCI and used the lowest 30 virtual spinors (instead of 19 spinors) as the valence spinors for LaF^+. The results are given in column 7 of Table 2. The calculated excitation energy to $(4f)_{7/2}^1$ becomes 2.16 eV. Agreement between this C4 calculation and experiment is reasonable. There is similar agreement between this and LFT calculations; the semiempirical parameters in LFT may implicitly include correlation effects between the valence and 4s, 4p, and 4d electrons as well as the 5s and 5p electrons.

We also found that the 19 virtual spinor sets give an unnaturally higher MC-QDPT solution in some states at smaller internuclear distances, but the 30 spinor set does not. Henceforth we use the C4 model with the lowest 30 virtual spinors of LaF^{2+}; the LaF^{2+} 145 DFR spinors are consequently divided into the 17 active core, 30 valence, and 98 virtual spinors of LaF^+.

3.1.3. Excited States and Their Spectroscopic Constants. Table 3 shows the assignment of the states, excitation energies, and spectroscopic constants by experiment, LFT, and C4 MC-QDPT. In the assignments, the approximate gross atomic orbital populations (GAOPs)[34] given by MC-QDPT are included in the form $(\lambda)^{GAOP\lambda}$ (λ = s, p, d, and f)

$$GAOP_\lambda = \sum_I C_I^2 GAOP_{I\lambda} \qquad (2)$$

where λ, I, and C_I respectively indicate the symmetry of the atomic spinor, configuration, and mixing configurational coefficient in MC-QDPT. The important configurations are also included in the assignment, where the numbers in the Slater determinant |...| are spinors given in Table 1; the spinors for the active-core are not shown, and a number with an underline such as "$\underline{i}$" indicates the Kramer's partner of the spinor "i". The weights of the main configurations for the zeroth−ninth states are always greater than 0.9 except for the fifth state, indicating that use of the virtual spinors of LaF^{2+} as the valence spinors of the ground and excited states of LaF^+ is adequate. Two excitation energies T_0 and T_e are listed. No experimental T_e values are known, but the calculated T_e values are quite close to the calculated T_0 values, which are themselves close to the experimental values.

We now discuss the f-excited states. One of the $(f)_{5/2}^1$ (the sixth excited state) remains at 1.86 eV above the ground state,

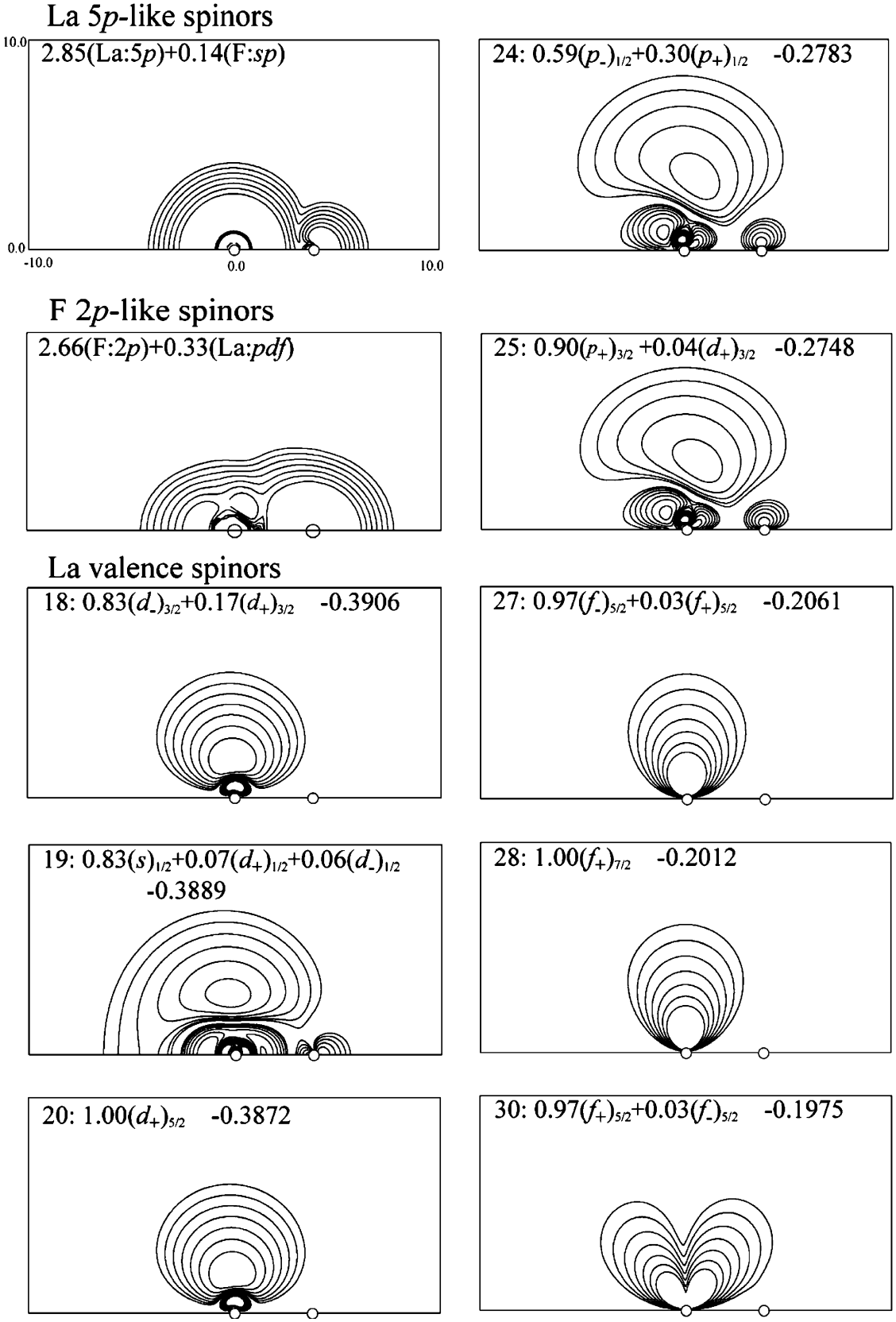

Figure 1. Contour maps of densities of the valence spinors of the ground state LaF^{2+}, together with spinor energies. The caption "*n*; $pop_1(l_\pm)_{\lambda/2}$ + $pop_2(l'_\pm)_{\lambda/2}$ ϵ" for the respective contour maps denotes the *n*th spinor having total electronic angular momentum $\lambda/2$, contributed largely from the La $l_\pm$ and $l'_\pm$ spinors having electronic populations pop_1 and pop_2 and followed by the spinor energy in hartrees. The horizontal and vertical (*z*- and *x*-) axes are in bohrs; *z* covers −10 to 10 bohrs, and *x* covers 0 to +10 bohrs. The circles on the *z*-axis at $z = 0.0$ and 3.783 bohrs (2.002 Å) indicate the La and F nuclei, respectively. The outermost values of the contour line are 0.0001 *e* $bohrs^{-3}$. The contour maps for La 5p and F 2p are the sum of those for (the 12th, the 13th, and the 14th) and for (the 15th, the 16th, and the 17th) spinors in Table 1. The value on a contour is twice that of the neighboring one outside it. The electron numbers inside the outermost line are between 0.956 and 1.001, except for the La 5p-like and F 2p-like spinors for which the electron numbers are 3.000 and 3.001, respectively. (For the former, contributions from La 5p are 2.852 and from others are 0.148; for the latter, contributions from F 2p are 2.659 and from others are 0.342.)

TABLE 2: Excitation Energies T_0 for LaF^+ (eV)[a]

assignment		C1	C2	C3	C4		results of others	
spnrs in CAS-CI		19	19	19	19	30		
exptl	prsnt	Cd+He	Pd + He	Kr + He	Zn^{2+}+ He		LFT[b]	exptl[c]
$^2\Delta_{3/2}$	$(d)_{3/2}^1$	0.000	0.000	0.000	0.000	0.000	0.000	0.000
$^2\Delta_{5/2}$	$(d)_{5/2}^1$	0.143	0.145	0.149	0.147	0.151	0.174	0.034
$^2\Phi_{5/2}$	$(f)_{5/2}^1$	3.315	3.070	2.544	2.097	1.862	1.996	2.050
$^2\Phi_{7/2}$	$(f)_{7/2}^1$	3.529	3.301	2.826	2.408	2.159	2.170	2.120
$^2\Pi_{1/2}$	$(pf)_{1/2}^1$	3.477	3.312	4.037	3.965	4.001	3.596	3.749
$^2\Pi_{3/2}$	$(pf)_{3/2}^1$	3.645	3.461	4.072	3.950	4.090	3.918	3.769

[a] Total energies for the ground state including zero-point vibrational energy are −8593.550669, -8593.595713, −8594.157965, and −8594.433519 hartrees for C1, C2, C3, and C4, respectively. [b]LFT stands for ligand field theory. See ref 2. [c]See ref 2.

TABLE 3: Assignments of States, Excitation Energies, and Spectroscopic Constants of LaF^+ by C4 MC-QDPT[a]

	exptl asgn[b]		prsnt asgn			T_0 (eV)			T_e(eV)	R_e (Å)		ω (cm^{-1})	
no.	sym	config	sym	GAOP	important CSF[c]	exptl[b]	LFT[b]	prsnt	prsnt	exptl[d]	prsnt	exptl[d]	prsnt
0	$^2\Delta_{3/2}$	d	3/2	$(d)^1$	1.00|18|+...	0.000	0.000	0.000	0.000	1.998	2.002	603.6	521.6
1	$^2\Delta_{5/2}$	d	5/2	$(d)^1$	0.85|20|-0.52|$\underline{20}$|+...	0.034	0.174	0.151	0.151	1.998	2.000	605.2	523.9
2			1/2	$(s)^{0.8}(d)^{0.1}$	0.94|$\underline{19}$|-0.30|$\overline{19}$|+...	.		0.293	0.288		1.966		612.4
3			1/2	$(p)^{0.1}(d)^{0.8}(f)^{0.1}$	0.70|$\overline{21}$|+0.66|21|+...			0.812	0.813		2.057		516.3
4			3/2	$(p)^{0.1}(d)^{0.8}(f)^{0.1}$	0.96|$\underline{22}$|-0.22|33|+...			0.902	0.903		2.056		516.2
5			1/2	$(s)^{0.1}(p)^{0.3}(d)^{0.4}(f)^{0.2}$	0.71|$\underline{23}$|+0.41|23|+0.38|$\underline{26}$|+...			1.533	1.530		2.054		570.7
6	$^2\Phi_{5/2}$	f	5/2	$(f)^1$	0.80|$\overline{27}$|-0.54|27|+...	2.050	1.996	1.862	1.863	2.065	2.078	555.8	514.3
7			3/2	$(f)^1$	0.81|$\overline{29}$|+0.52|29|+...			1.995	1.996		2.070		502.6
8	$^2\Phi_{7/2}$	f	7/2	$(f)^1$	0.93|$\overline{28}$|+0.29|$\underline{28}$|+...	2.120	2.170	2.159	2.159	2.065	2.080		516.4
9			5/2	$(f)^1$	0.71|30|-0.66|$\underline{30}$|+...			2.234	2.236		2.070		504.5
10			1/2	$(s)^{0.3}(p)^{0.2}(d)^{0.1}(f)^{0.3}$	0.59|$\underline{31}$|-0.56|$\overline{32}$|+...			2.482	2.483		2.096		517.1
11			3/2	$(p)^{0.2}(d)^{0.1}(f)^{0.7}$	0.86|$\overline{33}$|-0.39|$\overline{25}$|+...			2.572	2.574		2.083		507.4
12			1/2	$(s)^{0.1}(p)^{0.4}(d)^{0.2}(f)^{0.3}$	0.57|26|-0.45|23|-0.37|$\underline{26}$|+...			3.169	3.172		2.106		471.4
13	$^2\Pi_{1/2}$	p	1/2	$(s)^{0.1}(p)^{0.7}(d)^{0.1}(f)^{0.1}$	0.84|24|-0.32|$\underline{24}$|+...	3.749	3.596	4.001	3.993	1.976	1.971		647.0
14	$^2\Pi_{3/2}$	p	3/2	$(p)^{0.8}(d)^{0.1}(f)^{0.2}$	0.91|25|+0.39|$\overline{33}$|+...	3.769	3.918	4.090	4.082	1.976	1.968		666.0
15			1/2	$(s)^{0.1}(p)^{0.4}(d)^{0.1}(f)^{0.4}$	0.54|$\underline{34}$|+0.52|$\underline{26}$|+...			6.317	6.310		1.992		653.3
16			1/2	$(s)^{0.3}(p)^{0.2}(d)^{0.1}(f)^{0.4}$	0.61|$\overline{32}$|+0.56|$\underline{31}$|+...			6.923	6.907		1.976		789.4

[a] TEs with and without zero point vibrational energy are −8594.433519 and −8594.434718 hartrees, respectively. [b]See ref 2. [c]The numbers in a determinant |...| are the spinors given in Table 1, and a spinor (*i*) with an underbar indicates the Kramer's partner of (*i*). [d]See ref 1.

and the other $(f)_{5/2}^1$ (the ninth excited state) is at 2.23 eV above. Let us consider why this difference arises. The former state consists almost completely of 0.80|...$\underline{27}$| − 0.54|...27|, and the latter 0.71|...30| − 0.66|...$\underline{30}$|. From Figure 1, we see that the 30th spinor, $(4f_+)_{5/2}$-like, has a lobe where F 2p has significant density, causing the 30th spinor energy to be higher than that of the $(4f_-)_{5/2}$-like 27th spinor, and also the state with 30th to be energetically higher than 27th.

The potential curves are shown in Figure 3. If the CSF, including diffuse contributors such as the 19th, 24th, and 25th spinors characterized by the 6s and 6p atomic spinors (see Figure 1), has significant CI coefficient (as in the second, 13th, and 14th excited states in Table 3), then R_e becomes shorter than

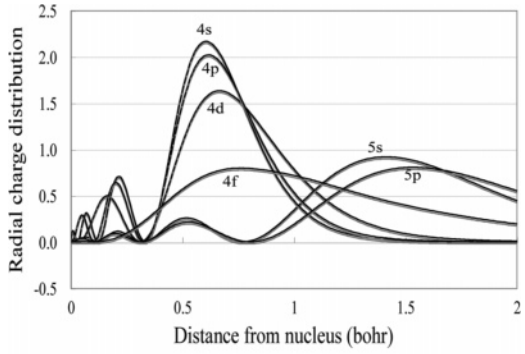

Figure 2. Charge distributions for atomic La 4s, 4p−, 4d−, 4f−, 5s, and 5p− spinors. The charge distributions of l_- and l_+ spinors for La-$(5p^6)^{3+}$ are close, so that we give l_- as representative. The spinors are those for $La(5p^6)^{3+}$ and the basis set for describing them is that of KTM.[19]

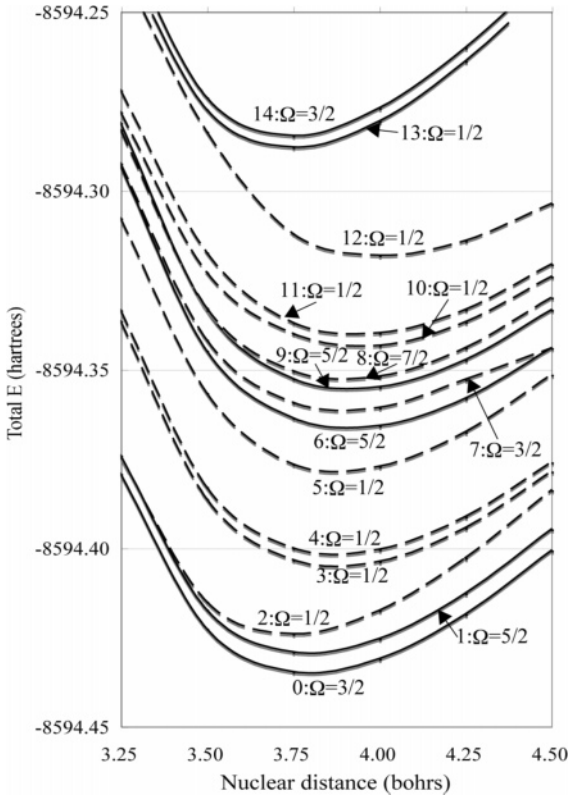

Figure 3. MC-QDPT potential curves for LaF^+. The solid and the dashed lines respectively indicate observed and unobserved states.

TABLE 4: Spinor Energies (hartrees) and GAOPS of LaF^+ at 2.052 Å with C4[a,b]

no.	spnr energy	Ω	La s_+	La p_-	La p_+	La d_-	La d_+	La f_-	La f_+	F s_+	F p_-	F p_+
10	−2.0677	1/2	1.958	0.000	0.000	0.000	0.000	0.000	0.000	0.034	0.003	0.006
11	−1.7182	1/2	0.034	0.046	0.061	0.005	0.006	0.002	0.002	1.826	0.006	0.012
12	−1.3564	1/2	0.001	1.919	0.016	0.001	0.000	0.000	0.000	0.042	0.001	0.021
13	−1.2616	3/2	0.000	0.000	1.990	0.000	0.000	0.000	0.000	0.000	0.000	0.010
14	−1.2539	1/2	0.003	0.004	1.825	0.001	0.003	0.000	0.000	0.077	0.045	0.042
15	−0.7883	1/2	0.000	0.008	0.007	0.042	0.037	0.019	0.017	0.000	1.321	0.550
16	−0.7860	3/2	0.000	0.000	0.016	0.016	0.063	0.010	0.026	0.000	0.000	1.868
17	−0.7825	1/2	0.014	0.028	0.082	0.071	0.091	0.015	0.018	0.008	0.481	1.192
	$\sum GAOP_{ii}(i = 1,17)$		4.010	4.004	7.997	4.136	6.199	0.046	0.062	1.987	1.857	3.701
	Total GAOP for a-core					La:26.454					F:7.547	
18	−0.4012	1/2	0.798	0.010	0.021	0.077	0.087	0.001	0.001	0.000	0.001	0.003
	Total GAOP for val					0.995					0.004	
19	−0.3809	1/2	0.005	0.101	0.029	1.112	0.618	0.061	0.038	0.000	0.022	0.015
20	−0.3433	1/2	0.154	0.186	0.326	0.348	0.753	0.072	0.124	−0.009	0.018	0.027
21	−0.2858	1/2	0.001	1.189	0.571	0.058	0.029	0.113	0.034	0.001	0.001	0.003
22	−0.2472	1/2	0.077	0.206	0.621	0.024	0.054	0.474	0.538	0.002	0.001	0.004
23	−0.2089	1/2	0.002	0.075	0.009	0.078	0.030	1.018	0.759	0.000	0.018	0.012
24	−0.1803	1/2	1.772	0.033	0.066	0.022	0.047	0.017	0.042	0.001	0.001	0.000
25	−0.1630	1/2	0.065	0.402	0.840	0.060	0.106	0.185	0.346	−0.034	0.011	0.019
26	−0.1617	3/2	0.000	0.000	0.001	1.664	0.329	0.005	0.001	0.000	0.000	0.000
27	−0.1592	5/2	0.000	0.000	0.000	0.000	1.994	0.001	0.005	0.000	0.000	0.000
28	−0.1442	1/2	0.000	1.335	0.643	0.003	0.002	0.011	0.006	0.000	0.000	0.001
29	−0.1430	3/2	0.000	0.000	0.720	0.189	1.036	0.009	0.025	0.000	0.000	0.022
30	−0.1262	1/2	0.004	0.026	0.073	0.260	1.119	0.008	0.512	−0.002	0.001	−0.001

[a] This is R_e of the LaF ground state from C4 MC-QDPT; the DFR total energy for LaF^+ is -8593.141760 hartree. [b]The lower first to ninth spinors and the higher 31st to 145th spinors are not shown to save space.

that of the ground state including tight 4f- and 5d-like spinors (see Figure 3 and Table 3). A dilute valence electron distribution leads to a stronger electrostatic interaction between the $La^{2.5+}$-$(5p^6d^{*0.4}f^{*0.1})$ and $F^{0.5-}(2p^{5.5})$ ions and to a shorter R_e. The calculated ω_e values have some scope for improvement.

In concluding the LaF^+ calculations, we derived the correct spectroscopic constants, including the excitation energies T_0. In considering the f spectra, we should pay special attention to the orientation of the f spinors. Electron correlations between the valence and the N shell were significantly as well as correlations between the valence and the O shell.

3.2. LaF. *3.2.1. LaF^+ DFR Spinors for CAS and MC-QDPT Calculations on LaF.* For LaF we used the model C4, where the frozen-core is $Zn^{2+}(28)$ and He(2). We performed RFCA DFR calculations for LaF^+, because LaF^+ provides an appropriate potential for the valence spinors for LaF, as LaF^{2+} does for LaF^+. The results for LaF^+ are shown in Table 4, and the contour maps for the important spinors are displayed in Figure 4. The LaF^+ 145 DFR spinors are divided into the 17 active core, 30 valence, and 98 virtual spinors of LaF. Contrary to experiment, $(6s_+)_{1/2}{}^1$ becomes the ground state in DFR, rather than $(5d)_{3/2}{}^1$ (see the 18th and 26th spinors in Figure 4); a valence electron $\{(s)_{1/2}{}^{0.8} + (d)_{1/2}{}^{0.2}\}$ moves in the field generated by $\{La^{2.6+}(5p^{6.0}d^{*0.3}f^{*0.1})F^{0.6-}(2p^{5.6})\}^{2+}$ as indicated in Table 4. The attractive potential of LaF^+ in the DFR model is not strong enough to maintain the electron in the 5d shell, and correlation effects are needed to attach the $(5d)_{3/2}$ electron to the LaF^{2+} core.

3.2.2. Excited States with $T_0 \leq 1.6$ eV and their Spectroscopic Constants. Using 30 LaF^+ valence spinors for the respective partners of the Kramer's pair, we performed CASCI and MC-QDPT calculations for LaF. Table 5 shows the assignments, excitation energies, and spectroscopic constants for states having $T_0 \leq 1.6$ eV. In the ground and single excited states having $c_1|18\underline{18}|$ or $c_1|18\underline{i}| + c_2|\underline{18}i|$, many have weights $(C_1{}^2$ or $C_1{}^2 + C_2{}^2) \geq 0.8$, indicating that use of the virtual spinors of LaF^+ as the valence spinors of the ground and excited states of LaF is adequate. Potential curves for the states with $T_0 \leq 1.6$ eV are shown in Figure 5.

Experimentally, the T_e values are well known but the T_0 values are not. The calculated T_0 values are close to the T_e values; the same may be true experimentally.

In the assignments, approximate GAOPs given by eq 2 and important configurations are included where the numbers in the determinant are the spinors in Table 6. We see no excited states with 4f spinors having a single electron. The ground state of LaF is written symbolically as $(6s)$,[2] but the GAOPs show that it is $6s^{1.4}6p^{0.1}5d^{0.5}$. As in experiment, the symmetry Ω is calculated as 0^+.

Within 0.3 eV above the ground state, three states are observed experimentally and are designated as $(6s^15d^1)\ ^3\Delta$ with $\Omega = 1$, 2, and 3. The present calculation reproduces these excitation energies with reasonable accuracy, and the GAOPs and Ω values support the experimental designation. We also confirm this assignment using the important CSFs in Table 5 and the shape of the d-mixed s-like 18th, pure d-like 26th and 27th spinors in Figure 4.

A small energy gap exists between the third and fourth excited states (see Table 5 and Figure 5). Experimentally, the fourth excited state is 0.39 eV from the third excited state; theoretically, it is 0.48 eV apart. The experimental and theoretical assignments are consistent.

The fifth to ninth excited states were designated experimentally as $(6s^15d^1)\ ^3\Pi$ and $^1\Pi$ with $\Omega = 0^-$, 0^+, 1, 2, and 1. The present work shows that the Ω's are correct but the experimental configurations are questionable, because the important CSFs and GAOPs in Table 5 suggest significant contributions from atomic p spinors; to see this, contrast the p-mixed d-like 19 and 29 spinors in the fifth to ninth excited states with the pure d-like 26 and 27 spinors in the first to fourth excited states (see Figure 4).

The 10th and 11th excited states are predicted theoretically to be around 1.46 eV above the ground state, but these are not found experimentally; the former is reported by Fahs and co-

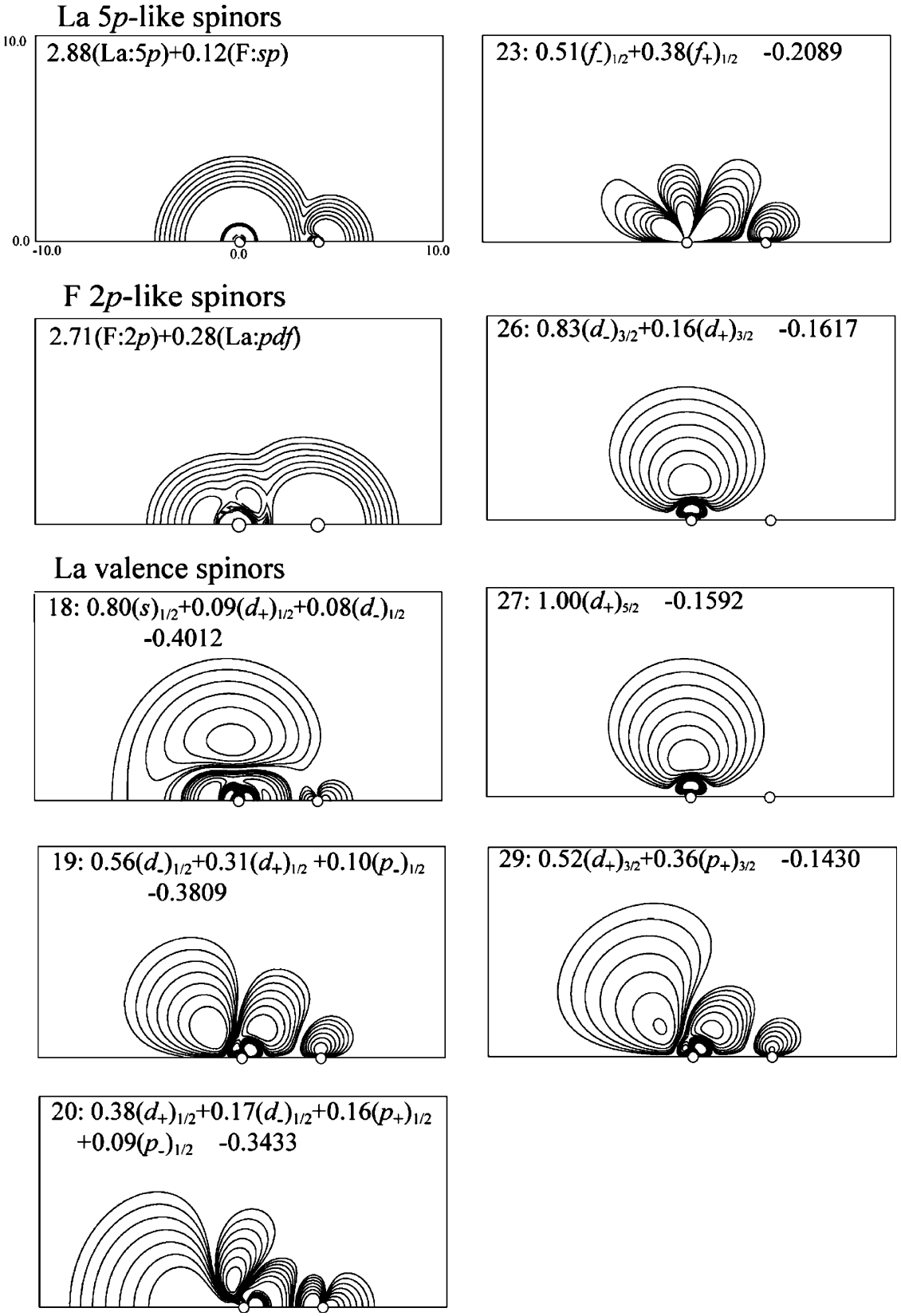

Figure 4. Contour maps of densities of the valence spinors of the ground state of LaF^+, together with spinor energies. The caption "*n*; $pop_1(l_\pm)_{\lambda/2}$ + $pop_2(l'_\pm)_{\lambda/2}$ ϵ", for the respective contour maps denotes the *n*th spinor having total electronic angular momentum $\lambda/2$, contributed largely from the La $l_\pm$ and $l'_\pm$ spinors having electronic populations pop_1 and pop_2 and followed by the spinor energy in hartrees. The horizontal and vertical (*z*- and *x*-) axes are in bohrs; *z* covers −10 to 10 bohrs and *x* 0 to +10 bohrs. The circles on the *z*-axis at $z = 0.0$ and 3.878 bohrs (2.052 Å) indicate the La and F nuclei, respectively. The outermost values of the contour line are 0.0001 *e* $bohrs^{-3}$. The contour maps for La 5p and F 2p are the sum of those for (the 12th, the 13th, and the 14th) and for (the 15th, the 16th, and the 17th) spinors in Table 4. The value on a contour is twice that of the neighboring one outside it. The electron numbers inside the outermost line are between 0.996 and 1.001, except for the La 5p-like and F 2p-like spinors for which the electron numbers are 3.000 and 3.001 respectively. (For the former, contributions from La 5p are 2.877 and from others are 0.123; for the latter, contributions from F 2p are 2.706 and from others are 0.295.)

TABLE 5: Assignment of States, Excitation Energies, and Spectroscopic Constants from C4 MC-QDPT for LaF Having $T_0 \leq 1.6$ eV[a]

	exptl asgn[b]				prsnt asgn			T_0 (eV)		T_e			R_e (Å)			ω (cm^{-1})		
no.	desig		Ω	config	Ω	GAOP	important CSF[c]	exptl	prsnt	exptl	Fahs[d]	prsnt	exptl	Fahs[d]	prsnt	exptl	Fahs[d]	prsnt
0	X	$^1\Sigma^+$	0^+	$6s^2$	0^+	$s^{1.4}p^{0.1}d^{0.5}f^{0.0}$	0.90*|18,18|+...		0.000	0.000[e]	0.000	0.000	2.023[e]	2.057	2.052	575.2[e]	583.3	533.5
1	a	$^3\Delta$	1	$6s^15d^1$	1	$s^{0.8}p^{0.0}d^{1.1}f^{0.0}$	0.78*|18,26|-0.57*|18,26|+...		0.216	0.180[f]	0.185	0.215	2.057[f]	2.095	2.085	541.2[f]	542.7	541.3
2	a	$^3\Delta$	2	$6s^15d^1$	2	$s^{0.8}p^{0.0}d^{1.1}f^{0.0}$	0.73*|18,26|-0.63*|18,27|+...		0.269	0.226[f]	0.234	0.268	2.055[f]	2.095	2.085	541.7[f]	543.2	543.0
3	a	$^3\Delta$	3	$6s^15d^1$	3	$s^{0.8}p^{0.0}d^{1.1}f^{0.0}$	0.71*|18,27|-0.66*|18,27|+...		0.340	0.288[f]	0.296	0.339	2.053[f]	2.095	2.084	542.9[f]	544.0	544.7
4	A'	$^1\Delta$	2	$6s^15d^1$	2	$s^{0.7}p^{0.1}d^{1.1}f^{0.0}$	0.64*|18,27|+0.53*|18,26|+...	0.679[d]	0.818		0.659	0.817		2.096	2.089	528.0[b]	537.7	546.5
5	b	$^3\Pi$	0^-	$6s^15d^1$	0^-	$s^{0.8}p^{0.2}d^{0.9}f^{0.1}$	0.64*|18,19|+0.64*|18,19|+...		0.972	0.816[g]	0.834	0.973	2.092[g]	2.116	2.118	511.6[g]	518.4	532.5
6	b	$^3\Pi$	0^+	$6s^15d^1$	0^+	$s^{0.8}p^{0.2}d^{1.0}f^{0.1}$	−0.64*|18,19|+0.64*|18,19|+...		0.979	0.821[g]	0.844	0.979	2.092[g]	2.116	2.117	511.6[g]	518.7	535.1
7	b	$^3\Pi$	1	$6s^15d^1$	1	$s^{0.8}p^{0.3}d^{0.8}f^{0.0}$	0.59*|18,29|+0.46*|18,29|+...		0.998	0.855[g]	0.880	0.998	2.092[g]	2.118	2.115	511.6[g]	516.9	536.8
8	b	$^3\Pi$	2	$6s^15d^1$	2	$s^{0.8}p^{0.4}d^{0.8}f^{0.0}$	0.73*|18,29|-0.57*|18,29|+...		1.081	0.917[g]	0.945	1.081	2.092[g]	2.119	2.113	511.6[g]	517.7	539.9
9	b	$^1\Pi$	1	$6s^15d^1$	1	$s^{0.6}p^{0.3}d^{1.1}f^{0.1}$	0.53*|18,19|-0.41*|18,19|+...		1.250	1.053[e]	1.103	1.250	2.109[e]	2.143	2.131	501.2[e]	505.8	536.6
10		$(^3\Sigma^+)$	(0^-)	$(6s^15d^1)$							1.465			2.141			494.4	
11		$(^3\Sigma^+)$	(1)	$(6s^15d^1)$	1	$s^{0.0}p^{0.0}d^{1.9}f^{0.0}$	0.74*|26,27|+0.63*|26,27|+...		1.457		1.467	1.458		2.144	2.115		499.4	515.7
12		$^3\Phi$	2		2	$s^{0.0}p^{0.4}d^{1.5}f^{0.1}$	0.59*|19,26|+0.50*|19,26|+...		1.633	1.355[f]		1.634	2.124[f]		2.144	474.0[f]	480.1	522.2
13		$^3\Phi$	3		3	$s^{0.0}p^{0.4}d^{1.6}f^{0.1}$	0.75*|26,29|+0.44*|19,27|+...		1.727	1.451[f]		1.729	2.125[f]		2.142	473.9[f]	476.7	509.0
14		$^1\Sigma^+$	0^+		0^+	$s^{0.0}p^{0.1}d^{1.9}f^{0.0}$	0.84*|26,26|-0.43*|27,27|+...	1.481[e]	1.402			1.402	2.107[e]		2.115			528.0
15		$^3\Phi$	4		4	$s^{0.0}p^{0.1}d^{1.8}f^{0.0}$	0.60*|26,27|-0.53*|26,27|+...	1.550[f]	1.813			1.816	2.116[f]		2.133			492.8

[a] TEs with and without zero-point vibrational energies are −8594.641557 and −8594.642772 hartrees, respectively. [b] See ref 4. [c] The numbers in a determinant |...| are the spinors given in Table 4, and a spinor (i) with an under bar indicates the Kramer's partner of (i). [d] See ref 15. [e] See ref 9. [f] See ref 10. [g] See ref 11.

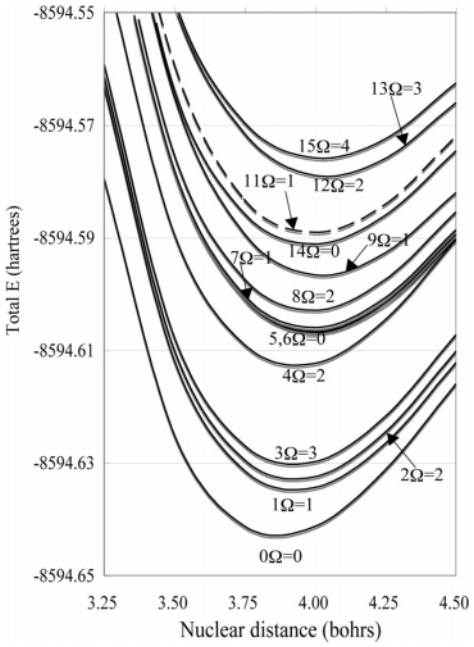

Figure 5. MC-QDPT potential curves for LaF ground and excited states with $T_0 \leq 1.6$ eV. The solid and the dashed lines, respectively, indicate observed and unobserved states. The 10th state is not given, because the state is predicted theoretically by Fahs and co-workers[15] but no corresponding state is found by the present calculation.

workers,[15] but is not shown in Figure 5. The 12th, 13th, and 15th excited states lie experimentally at 1.36, 1.45, and 1.55 eV above the ground state, respectively, and are designated as $^3\Phi$ with $\Omega = 2$, 3, and 4, but the electronic configurations are not given. The calculated values are 1.63, 1.73, and 1.81 eV above the ground state, and the electron configuration suggested by GAOPs are $6p^{0.4}5d^{1.5}4f^{0.1}$, $6p^{0.4}5d^{1.6}4f^{0.1}$, and $6p^{0.1}5d^{1.8}$ with $\Omega = 2$, 3, and 4. The configurations given are reasonable, because the states are mainly spanned with determinants composed of (the p-mixed d-like 19 and pure d-like 26), (the p-mixed d-like 29/19 and pure d-like 26/27), and (the pure d-like 26 and pure d-like 27) spinors. The 14th state, found experimentally at 1.48 eV, is designated as $^1\Sigma^+$ with $\Omega = 0^+$; this is a pure $(5d)^2$-like state having $71\%(5d)_{3/2}{}^2 + 18\%(5d)_{5/2}{}^2$.

We now discuss the spectroscopic constants. The calculated R_e for the ground state is 2.052 Å, and the experimental value is 2.023 Å. The experimental and calculated R_e values agree well. We may find that as the states becomes higher, the 6s GAOP decreases (see Table 5), and the excited state R_e increases (see Figure 5). The larger occupation in the diffuse 6s (see Figure 4) enhances the interaction between the $La^{2.6+}(5p^{6.0}d^{*0.3}4f^{*0.1})$ and $F^{0.6-}(2p^{5.6})$ ionic cores, leading to smaller R_e values.

The calculated ω_e values tend to decrease as the state becomes higher. Further investigation would be necessary to consider ω_e for the ground state for which the calculated ω_e is slightly smaller.

In conclusion, for the states with $T_0 \leq 1.6$ eV we see good correspondence between the present calculations, LFT,[15] and experiment, at least for T_0 and T_e. However, the assigned electronic configurations show some discrepancy, as in the fifth to ninth excited states where 6p(p*) occupations are considerable.

3.2.3. Excited States with 1.6 < T_0 ≤ 2.8 eV and Their Spectroscopic Constants. Assignments and spectroscopic constants for states having $1.6 < T_0 \leq 2.8$ eV are shown in Table 6. Again, we have no excited states with 4f spinors having a single electron occupation. The f-excited states may appear in the low-energy region, but only if the n (>1) electron ground state includes f spinor(s).

We now discuss the 16th to 19th excited states. Three of these four are found experimentally to remain in the range, at 1.60, 1.61, and 1.62 eV above the ground state. The experimental assignments are $^3\Pi$ with $\Omega = 0^+$, 0, and 2. Our investigation indicates that the excitation energies for 0^+ and 0^- are 1.68 and 1.63 eV, respectively. The Ω values are the same as experiment, and the calculated excitation energies are close to experiment. The experimental assignment suggests that the states at 1.60 and 1.61 eV have the same configuration because they both arise from $^3\Pi$, but the present calculation suggests that the two states do not have the same configuration, as seen in Table 6; the lower is $(spf)^{0.6}(d)^{1.5}$ and the higher is $(spf)^{1.3}(d)^{0.7}$. We also cannot find the state 1.62 eV with $\Omega = 2$; instead, we find the excited state with $\Omega = 1$ at 1.63 eV above the ground state. This state might be observed if a further experiment is performed.

In the 20th to 30th states, the agreement between the experimental and calculational excitation energies is good except for the 28th excited state having $\Omega = 4$; we doubt that MC-QDPT works appropriately for this state. Contrary to experiment, the 26th and 28th states tend to have $5d^2$ instead of the experimental configuration $5d^16p^1$ (see the important CSF in

TABLE 6: Assignment of States, Excitation Energies, and Spectroscopic Constants from C4 MC-QDPT for LaF Having 1.6 < $T_0 \leq$ 2.8 eV[a]

	exptl asgn			prsnt asgn			T_0 (eV)		T_e (eV)			R_e (Å)			ω (cm^{-1})		
no.	desig	Ω	config.	Ω	GAOP	important CSF[c]	exptl	prsnt	exptl	Fahs[b]	prsnt	exptl	Fahs[b]	prsnt	exptl	Fahs[b]	prsnt
16	$^3\Pi$	0^+		0^+	$s^{0.3}p^{0.2}d^{1.5}f^{0.1}$	0.71*|27,27|+0.36*|18,20|-0.36*|18,20|+...	1.601[f]	1.682		1.626	1.682		2.149	2.127		471.4	533.1
17	$^3\Pi$	0		0^-	$s^{0.8}p^{0.3}d^{0.7}f^{0.2}$	0.63*|18,20|+0.63*|18,20|+...	1.605[f]	1.630		1.628	1.631		2.149	2.136		470.5	524.4
18	$^3\Pi$	1		1	$s^{0.8}p^{0.3}d^{0.7}f^{0.2}$	0.72*|18,20|+0.53*|18,20|+...		1.634		1.641	1.635		2.148	2.138		472.1	527.3
19	$^3\Pi$	2					1.619[b]			1.646			2.147			473.2	
20				0^-	$s^{0.0}p^{0.4}d^{1.5}f^{0.0}$	0.66*|26,29|+0.66*|26,29|+...		1.909			1.910			2.147			510.0
21	c $^3\Delta$	1		1	$s^{0.0}p^{0.4}d^{1.5}f^{0.1}$	0.65*|27,29|+0.55*|19,26|+...	1.861[d]	1.923	1.868[e]		1.925	2.147[e]		2.155	448.0[e]		502.5
22	b $^3\Delta$	2		2	$s^{0.1}p^{0.3}d^{1.5}f^{0.1}$	0.70*|19,27|+0.48*|21,27|+...	1.876[d]	1.973			1.974			2.164			515.5
23	B $^1\Pi$	1	$5d^{2,e}$	1	$s^{0.5}p^{0.7}d^{0.7}f^{0.1}$	0.60*|18,21|+0.38*|27,29|+...	2.007[e]	2.166	2.011[e]		2.169	2.095[e]		2.159	505.7[e]		477.7
24		0^+	$5d^{2,e}$	0^+	$s^{0.0}p^{0.4}d^{1.5}f^{0.0}$	0.66*|26,29|-0.66*|26,29|+...	2.063[e]	1.914	2.071[e]		1.916	2.088[e]		2.146	440.0[e]		503.4
25	d $^3\Phi$	2	$5d^16p^{1,g}$	2	$s^{0.7}p^{0.6}d^{0.6}f^{0.1}$	0.84*|18,32|-0.21*|18,29|+0.20*|19,27|+...	2.446[g]	2.229			2.233			2.158			462.1
26	d $^3\Phi$	3	$5d^16p^{1,g}$	3	$s^{0.1}p^{0.3}d^{1.5}f^{0.2}$	0.66*|20,27|+0.39*|19,27|+...	2.520[g]	2.230			2.235			2.143			458.6
27	C $^1\Pi$	1		1	$s^{0.1}p^{0.3}d^{1.4}f^{0.2}$	0.64*|20,26|-0.53*|20,26|+...	2.599[d]	2.463			2.462			2.061			554.6
28	d $^3\Phi$	4	$5d^16p^{1,g}$	4	$s^{0.0}p^{0.3}d^{1.7}f^{0.0}$	0.76*|27,29|+0.52*|26,27|+...	2.618[g]	1.919			1.918			2.118			555.7
29	D $^1\Sigma$			0^+	$s^{0.7}p^{0.8}d^{0.4}f^{0.1}$	0.60*|18,21|-0.60*|18,21|+...	2.789[d]	2.410			2.412			2.047			506.3
30	E $^1\Sigma$			0^-	$s^{0.7}p^{0.8}d^{0.4}f^{0.1}$	0.62*|18,21|+0.62*|18,21|+...	2.799[d]	2.419			2.419			2.042			534.3

[a] TEs with and without zero point vibrational energies are −8594.641557 and −8594.642772 hartrees, respectively. [b]See ref 15. [c]The numbers in a determinant |...| are the spinors given in Table 4, and a spinor ($\underline{i}$) with an underbar indicates the Kramer's partner of (i). [d]See ref 4. [e]See ref 5. [f]See ref 7. [g]See ref 8.

TABLE 7: GAOPs at Corresponding R_e and Spectroscopic Constants of LaF^+ and LaF calculated with MC-QDPT

spinor	La s_+	La p	La d	La f	F s_+	F p
LaF^+ $\sum GAOP_i(i = 1,17)$	4.01	11.99	10.42	0.12	1.99	5.47
a-core: $La^{2.5+}(d^*)^{0.4}(f^*)^{0.1}$ $F^{0.5-}(2p)^{5.5}$		La: 26.53			F: 7.47	
valence: $5d^1$	0.00	0.00	1.00	0.00	0.00	0.00
spectroscopic constant[a]	R_e 2.002Å, ω_e 522 cm^{-1}, D_e 5.86(-[b]) eV					
LaF $\sum GAOP_{il}(i = 1,17)$	4.01	12.00	10.34	0.11	1.99	5.56
a-core: $La^{2.6+}(d^*)^{0.3}(f^*)^{0.1}$ $F^{0.6-}(2p)^{5.6}$		La: 26.45			F: 7.55	
valence $s^{1.4}p^{0.1}d^{0.5}f^{0.0}$	1.38	0.11	0.48	0.02	0.00	0.00
spectroscopic constant[c]	R_e 2.052Å, ω_e 534 cm^{-1}, D_e 5.72 (6.23[d]) eV					

[a] The MC-QDPT dissociation energy is calculated using the $C_{\infty v}$ double group: TE(LaF^+:Ω; 3/2, R;2.002 Å) = −8594.434718, TE(La^+:Ω;2) = −8494.527860, and TE(F:Ω; 1/2) = −99.691523 hartrees. [b]No experimental data are available. [c]The MC-QDPT dissociation energy is calculated using the $C_{\infty v}$ double group: TE(LaF:Ω;0^+, R;2.052 Å) = −8594.642772, TE(La:Ω;3/2) = −8494.740356, and TE(F:Ω;3/2) = −99.692041 hartrees. [d]Experimental value cited in ref 14.

Table 6; for example, the 26th state is composed of |p-mixed 20th, pure d-like 27th| and |p-mixed 19th, pure d-like 27th|).

The calculated ω_es and the experimental values do not agree very well, and warrant further investigation of the potential curves for the higher states.

So far we have discussed mainly the excited states of LaF^+ and LaF. We finally discuss the characteristics of the chemical bond in the ground state of LaF^+ and LaF.

3.3. Chemical Bond in LaF^+ and LaF. Table 7 summarizes the MC-QDPT GAOPs and spectroscopic constants for the ground states of LaF^+ and LaF. The ion cores for LaF^+ and LaF are almost $\{La^{2.5+}(5p^6d^{*0.4}f^{*0.1})F^{0.5-}(2p^{5.5})\}^{2+}$. The valence electrons are almost entirely located at $La^{2.5+}$in both LaF^+ and LaF.

For the LaF^+ ground state $^2\Delta$ ($\Omega = 3/2$), the valence electron is in the atomic-like La 5d spinor. The attraction potential in $La^{2.5+}$ $F^{0.5-}$ is not strong enough to hold the 4f electron but not so weak as to hold the 6s electron; recall that if the nuclear attraction is very strong compared to the electron−electron repulsion, the $4d_{5/2}$ and $4f_{5/2}$ are degenerate, and in this case the electron is naturally captured in 4f.

For the LaF ground state X $^1\Sigma^+$ ($\Omega = 0^+$), two electrons are located at the $La^{2.5+}$ having strong s-d hybridizations. The attraction potential in the ground state given by $(La^{2.5+}F^{0.5-})^{2+}$ is not strong enough to hold two 5d-like electrons as the La^{3+}-$(5p^6)$ core in the gaseous La^+ ion and is also not strong enough to keep one electron in the 6s and the other in the 5d spinor (we find many low lying ($6s^15d^1$) states instead, as was discussed).

We conclude that the chemical bond in LaF^+ and LaF is constructed through a formation of $\{La^{2.5+}(5p^6d^{*0.4}f^{*0.1})$-$F^{0.5-}(2p^{5.5})\}^{2+}$, which arises from the interaction between $La^{2+}(5p^65d^1)$ and $F(2p^5)$ (see the F 2p- and La 5p-like spinors in Figures 1 and 4), forcing valence electron(s) to move around $La^{2.5+}(5p^6d^{*0.4}f^{*0.1})$. In that case, the spectroscopic constants, R_e and ω_e, should be similar for LaF^+ and LaF, as should be the dissociation energies D_e. The spectroscopic constants in Table 7 confirm this; the values of D_e for LaF^+ and LaF are respectively 5.86 and 5.74 eV. The augmented electron in LaF^+, which is located at La, is responsible for the reduction in the total energy, giving the positive electron affinity (5.66 eV) for LaF^+ with only a small change in the molecular shape. A similar result was obtained by Franzreb and co-workers, using a nonrelativistic density functional approach.[35]

We believe that the formal charges for +1 and −1 for the La and F ions are reasonable, because the electrons in F^- flow partly back to La through d* and f*, and by treating the GAOPs for these orbitals as F^- the charges on F become −0.99 (GAOPs in Table 6).

Finally, we discuss the validity of the LFT calculations. The present calculation shows why the valence electron(s) localize-(s) at La. We can therefore discuss the electronic structure of the molecules by considering only the valence electrons, provided one can properly account for the correlation effects between the valence electrons and the $La^{2.5+}F^{0.5-}$ ion cores in various empirical parameters. Our discussion gives support to the LFT calculations.

4. Conclusion

We have used the RFCA four-component DFR method, CASCI, and MC-QDPT to study the electronic structures of the LaF^+ and LaF molecules.

The calculated excitation energies for LaF^+ agree with the experimental values; the errors are within 0.4 eV. For example, the highest observed state $^2\Pi$ is 3.77 eV above the ground state, and the calculated $^2\Pi$ is 4.09 eV above. The calculated excitation energies also agree with those of LFT, indicating that the empirical parameters in LFT implicitly include correlation effects between the valence and core electrons. When considering f spectra, we paid attention to the orientation of the f spinors.

For LaF, 30 states having excitation energy ≤ 2.80 eV were discussed. The excitation energies (and the angular momentum Ω) given by experiment and calculation agree to within 0.4 eV except for a single anomaly, but in some cases the electron configurations do not. In such cases, we have confidence in our assignment, especially in the lower excited states. The spectroscopic constants have also been considered.

The characteristics of the chemical bonds in LaF^+ and LaF have been discussed in detail. Common features in the ground state of LaF^+ and LaF are the following: (1) interaction between $La^{2+}(5p)^6(5d)^1$ and $F(2p)^5$ determines the electronic structure framework of the two molecules, forming $\{La^{2.5+}(5p^6d^{*0.4}f^{*0.1})$-$F^{0.5-}(2p^{5.5})\}^{2+}$; and (2) the valence electron(s) are almost completely localized at the La atom, because the positive ionic core of La attracts the electrons and the negative charges of F^- repel the additional electrons in the region of F^-. This second point validates the LFT calculations.

Acknowledgment. Calculations were performed using IBM p650 processors in the Library and Information Processing Center of Nagoya City University. The present work was supported by a Grant-in-Aid from the Ministry of Education, Culture, Sport, Science, and Technology (MEXT) of Japan.

References and Notes

(1) Shenyavskaya, E. A.; Gurvich, L. V. *J. Mol. Spectrosc.* **1980**, *81*, 152.

(2) Kaledin, L. A.; Kaledin, A. L.; Heaven, M. C. *J. Mol. Spectrosc.* **1996**, *179*, 246.

(3) Barrow, R. F.; Bastin, M. W.; Moore, D. L. G.; Pott, C. J. *Nature* **1967**, *215*, 1072.

(4) Schall, H.; Linton, C.; Field, R. W. *J. Mol. Spectrosc.* **1983**, *100*, 437.

(5) Kaledin, L. A.; Kaledin, A. L.; Heaven, M. C. *J. Mol. Spectrosc.* **1997**, *182*, 50.

(6) Simard, B.; James, A. W. *J. Chem. Phys.* **1992**, *97*, 4669.

(7) Verges, J.; Effantin, C.; d'Incan, J.; Bernard, A.; Shenyavskaya, E. A. *J. Mol. Spectrosc.* **1999**, *198*, 196.

(8) Kaledin, L. A.; McCord, J. E.; Heaven, M. C. *J. Opt. Soc. Am. B* **1994**, *11*, 219.

(9) Bernard, A.; Effantin, C.; d'Incan, J.; Verges, J. *J. Mol. Spectrosc.* **2000**, *202*, 163.

(10) Bernard, A.; Effantin, C.; d'Incan, J.; Verges, J. *J. Mol. Spectrosc.* **2000**, *204*, 55.

(11) Bernard, A.; Effantin, C.; Shenyavskaya, E. A.; d'Incan, J. *J. Mol. Spectrosc.* **2001**, *207*, 211.

(12) Balasubramanian, K. *Handbook on the Physics and Chemistry of Rare Earths*; Eyring, L, Ed.; Elsevier: New York, 2003; Vol. 18; p 29.

(13) Schall, H.; Dulick, M.; Field, R. W. *J. Chem. Phys.* **1987**, *87*, 2898.

(14) Hong, G.; Dolg, M.; Li, L. *Chem. Phys. Lett.* **2001**, *334*, 396.

(15) Fahs, H.; Allouche, A. R.; Korek, M.; Aubert-Frécon, M. *J. Chem. Phys.* **2002**, *117*, 3715.

(16) Matsuoka, O. *J. Chem. Phys.* **1992**, *96*, 6773.

(17) Watanabe, Y.; Matsuoka, O. *J. Chem. Phys.* **1998**, *109*, 8182.

(18) Huzinaga, S.; Andzelm, J.; Klobukkowski, M.; Radzio-Andzelm, E.; Sakai, Y.; Tatewaki, H. *Physical Science Data 16, Gaussian Basis Sets for Molecular Calculations*; Elsevier New York, 1984.

(19) Koga, T.; Tatewaki, H.; Matsuoka, O. *J. Chem. Phys.* **2002**, *117*, 7813.

(20) Koga, T.; Tatewaki, H.; Matsuoka, O. *J. Chem. Phys.* **2001**, *115*, 3561.

(21) Brown, G. E.; Ravenhall, D. G. *Proc. R. Soc. London, Ser. A* **1951**, *208*, 552.

(22) Mittleman, M. H. *Phys. Rev. A* **1971**, *4*, 893.

(23) Sucher, J.; *Phys. Rev. A* **1980**, *22*, 348.

(24) Hardekopf, G.; Sucher, J. *Phys. Rev. A* **1984**, *30*, 703.

(25) Hess, B. A.; *Phys. Rev. A* **1986**, *33*, 3742.

(26) Visscher, L. *Relativistic Electronic Structure Theory, part I. Fundamentals*; Schwerdtfeger, P. Ed.; Elsevier, New York, 2002; p 291.

(27) Roos, B. O.; Taylor, P. R.; Siegbahn, P. E. M. *Chem. Phys.* **1980**, *48*, 157.

(28) Miyajima, M.; Watanabe, Y.; Nakano, H. *J. Chem. Phys.* **2006**, *124*, 044101.

(29) Schucan, T. H.; Widenmüller, H. *Ann. Phys.* **1972**, *73*, 108−35.

(30) Sheppard, M. G.; Freed, K. F. *J. Chem. Phys.* **1981**, *75*, 4507.

(31) Witek, H. A.; Choe, Y-K.; Finley, J. P.; Hirao, K. *J. Comp. Chem.* **2002**, *23*, 957.

(32) Numerov, B. *Publ. Obs. Cent. Astrophys. Russ.* **1933**, *2*, 188.

(33) Thijssen, J. M. *Computational Physics*; Cambridge, 1999.

(34) Mulliken, R. S. *J. Chem. Phys.* **1955**, *23*, 1833.

(35) Franzreb, K.; Hrusák, J.; Alikhani, M. E.; Lörincík, J.; Sobers, R. C., Jr.; Williams, P. *J. Chem. Phys.* **2004**, *121*, 12293.